GEOPHYSICAL RESEARCH LETTERS, VOL. 27, NO. 19, PAGES 3093-3096, OCTOBER 1, 2000

Ground deformation near Gada 'Ale Volcano, Afar, observed by Radar Interferometry

Falk Amelung[1]
Geophysics Department, Stanford University, Stanford, USA

Clive Oppenheimer
Department of Geography, Cambridge, U.K

P. Segall and H. Zebker
Geophysics Department, Stanford University, Stanford, USA

Abstract. Radar interferometric measurements of ground-surface displacement using ERS data show a change in radar range, corresponding to up to 12 cm of subsidence near Gada 'Ale volcano in northern Afar, Ethiopia, that occurred between June 1993 and May 1996. This is the area of lowest topography within the Danakil Depression (-126 m). Geodetic inverse modeling and geological evidence suggest a volcanic origin of the observed deformation; it was probably caused by a combined process of magma withdrawal from a larger reservoir and normal faulting. There is no evidence of subaerial eruption. This is the only identifiable deformation event during June 1993-October 1997 in the 80 km long Erta 'Ale volcanic range, indicating surprising inactivity elsewhere in the range.

Introduction

The Afar Triangle is the region where the Nubian, Somalian, and Arabian plates meet above a mantle plume [*White et al.*, 1989]. The oceanic ridges in the Red Sea and Gulf of Aden do not connect directly but appear to have propagated onshore into Afar. This is expressed in the north by the 80-90 km long, 30 km wide axial volcanic range of Erta 'Ale and in the southeast by the Asal Rift (Fig. 1) [*Manighetti et al.*, 1997]. Recent activity in this area include a dike intrusion near the Asal rift [*Tarantola et al.*, 1979], contemporary volcanism in the Manda Inakir and Manda Hararo rifts [*Tapponnier et al.*, 1990], and strike-slip and normal faulting in the overlap area between these two rift zones [*Tapponnier et al.*, ibid., *Sigmundsson*, 1992].

The regional deformation of the Danakil Depression, a well defined topographic basin within north Afar (Fig. 1), has been modeled as a counter-clockwise rotation of the Danakil microplate with respect to the Nubian plate about an Euler pole ~250 km NNW of Erta 'Ale [*Chu and Gordon*, 1998]. This explains the southward increase in depression width and volcanism, the latter manifested in the basaltic shields of Alayta, Afdera, Barawli, and Erta 'Ale (Fig. 1). The lack of extrusive volcanism further north suggests that crustal thinning has not yet reached a state that allows penetration of magma in this deepest part of Danakil (-126 m) [*Barberi and Varet*, 1970].

The aim of this work is to identify (using InSAR) ground deformation on the largest of the axial volcanic ranges in the Danakil - the Erta 'Ale range. We anticipated finding deformation in the center of the range associated with the active lava lake at Erta'Ale volcano [*Oppenheimer and Francis*, 1998]. Instead, we observed deformation at the northern tip of the range, near Gada 'Ale volcano (Fig. 2).

Observational Data

Few ERS SAR images of the Erta 'Ale range have been acquired. We formed an interferogram spanning 4.3 yr using images acquired on 29 June 1993 and 9 Oct, 1997, a 1.4 yr interferogram using images acquired on 3 May 1996 and 10 Oct. 1997, and a 1 day interferogram using the 1997 images. The perpendicular baselines between image acquisitions were 205 m, 330 m, and 364 m, respectively. We used the 1.4 yr interferogram for the removal of topography because the differential interferogram obtained using the 1 day interferogram had significant atmospheric disturbances probably introduced by the common 9 October SAR image. In Afar atmospheric water vapor heterogeneity results in local signal delays of typically 1-2 phase cycles (2.8-5.6 cm range displacement). This makes it impossible to see subtle sub-centimeter scale deformation that has been detected under optimal atmospheric conditions [*Amelung et al.*, 1999]. For recent reviews of volcano applications of InSAR see *Massonnet and Feigl* [1998], *Massonnet and Sigmundsson* [2000], and *Zebker et al.* [2000].

Across the whole of the Erta 'Ale range, we detected significant ground deformation only at the northernmost part between Gada 'Ale volcano (+260 m) and Lake Karum (-126 m, Figs. 2, 3). About four fringes in the interferogram in a 4 km^2 area represent an increase in ground-to-radar distance of up to 11 cm between the two image acquisitions. Ground deformation clearly extends under Lake Karum where measurements are unavailable. The incidence angle of the radar is 23°. The fringes may be caused by 12 cm of local subsidence, by 30 cm of horizontal E displacement, or by a combination of both. The bare volcanic rocks maintain high coherence of the radar signal. The continuity of the phase in the interferogram indicates the lack of significant surface breaks. The fringes are round, smooth and isolated, typical of elastic deformation. This, together with the lack of any comparable phase signature in the entire 100 x 100 km^2 interferogram,

[1]Now at Hawaii Institute of Geophysics and Planetology, University of Hawaii, Honolulu, USA.

Paper number 2000GL008497.
0094-8276/00/2000GL008497$05.00

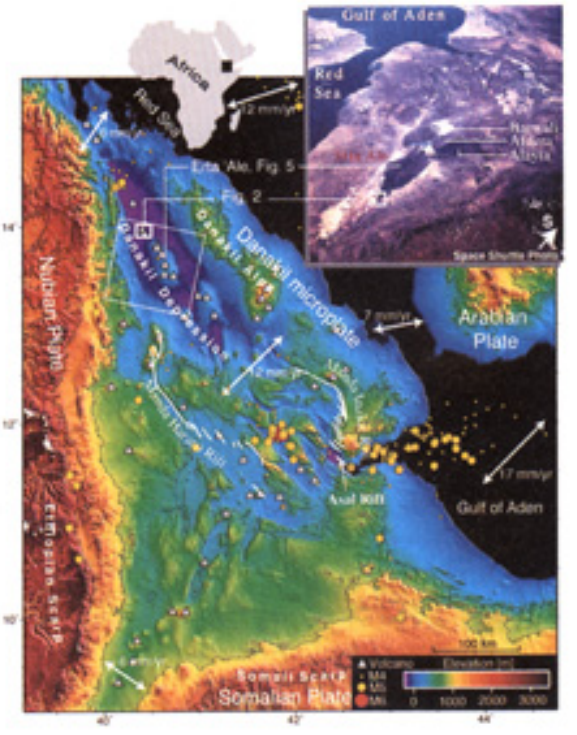

Figure 1. Topography of Afar showing major tectonic features, earthquakes 1971-1998 (NEIC), active volcanoes, and area covered by ERS SAR scene. Arrows indicate plate motion between Nubia and Somalia, Somalia and Arabia, Nubia and Danakil, Danakil and Arabia, determined from Euler poles and angular velocities by *Chu and Gordon* [1998]. Rifts (names simplified) redrawn from *Tapponnier et al.* [1990]. Inset shows Space Shuttle photograph looking SE.

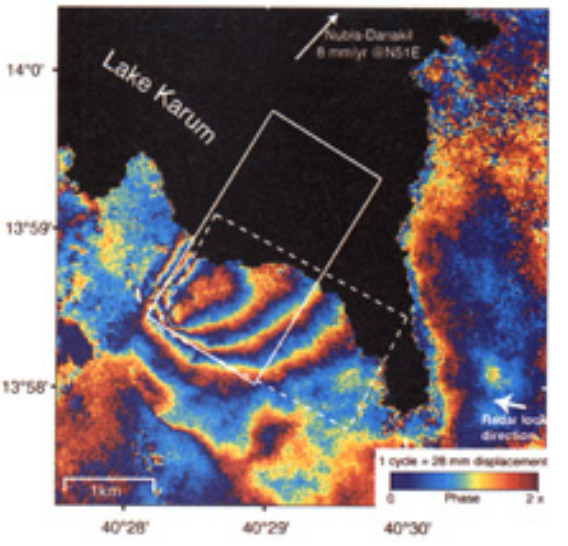

Figure 3. June 1993 - Oct. 1997 interferogram for Gada 'Ale area. One cycle of phase corresponds to 2.8 cm change in ground-to-radar distance. Surface projections of model A (solid line) and model B (dashed line) are also shown.

makes us confident that we are observing real deformation and not atmospheric disturbance. However, because we lack a second 1992/93 SAR image we cannot definitively exclude an artifact using *Massonnet and Feigl's* [1998] image-pair logic.

The precise timing of the observed deformation is uncertain because it cannot be related to any recorded seismicity. Only one moderate earthquake occurred in the Erta 'Ale range during 1971-99 (M4.9 in 1989 at 13°46'N, 40°36'E, Fig. 1), suggesting that crustal extension in Danakil is largely aseismic (the detection threshold of the NEIC catalogue is ~M4.5). It is unlikely that a slow, continuous process occurred because the 1.3 yr interferogram lacks a similar phase signature.

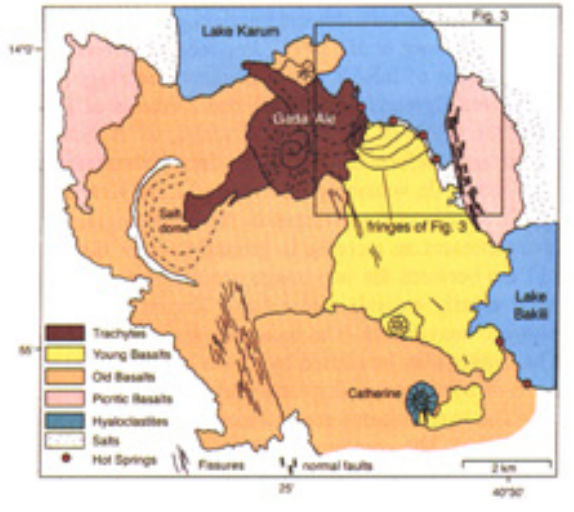

Figure 2. Simplified geologic map of the northern Erta 'Ale range after *Barberi and Varet* [1970]. Holocene volcanism occurred on NNE fissures southeast of Gada 'Ale.

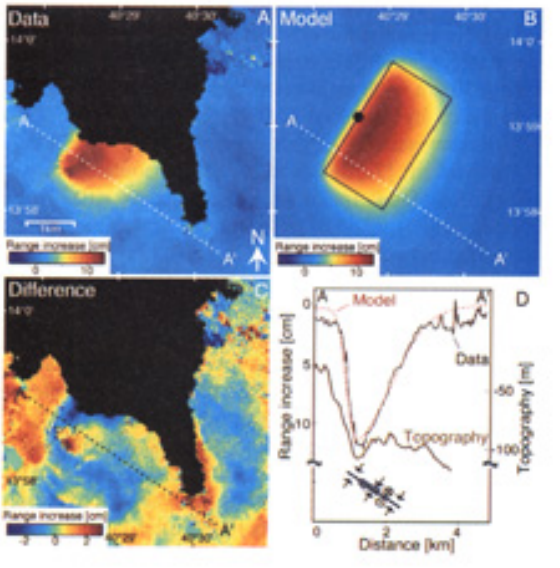

Figure 4. **A** Measured range displacements (phase unwrapped). **B** Best-fitting dislocation (model A, Table 1, solid line is surface projection). **C** Difference data minus model. **D** Data and model range displacements along Profile AA' together with topography and source. Profile through model vertical displacement is similar to profile through model range displacement.

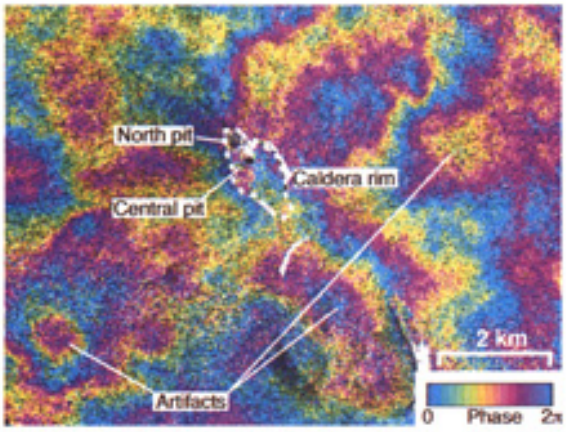

Figure 5. June 1993 – Oct 1997 interferogram for Erta 'Ale volcano. The north and central pits have active lava lakes.

Modeling the Data

We assume that the observed deformation was caused by a uniform dislocation on a finite rectangular surface in an elastic, Poisson medium, described by ten parameters (Okada, 1985): length, width, strike, and dip of the dislocation surface, three parameters for the location, and the strike-slip, down-dip and opening components of the dislocation vector. This model includes shear faults (earthquakes) with the opening component of the displacement vector zero, and dikes and sills with the strike-slip and dip-slip components of the dislocation vector zero.

The best-fitting model minimizes the root mean square of differences (rms) between the data and model predictions. The data consist of 619 range displacement measurements obtained from the interferogram after unwrapping the phase (measured modulo 2π), and applying a median filter to 7 x 7 pixel areas of the interferogram (20,000 m^2). Model range displacements are obtained by projecting the surface-displacement vector into the radar-look direction (0.42, -0.09, 0.90). To solve this non-linear optimization problem we first use a Monte Carlo simulated annealing algorithm to locate the area in model space containing the global minimum and then a quasi-Newton method to exactly locate the minimum in this area [*Cervelli et al.,* 2000]. We assume uncorrelated data.

The best-fitting dislocation has 4.9 km^2 surface area, is very shallow (0.2 – 1.2 km), strikes NNE, and dips shallowly (36°) to the ESE (Fig. 4, Model A in Table 1). The components of the dislocation vector are 4 cm of left-lateral strike-slip, 18 cm of normal slip, and 9 cm of collapse. This model explains most of the signal except in the area of maximum range displacement at 13°58.5'N, 40°28.3'E (Fig. 4C). The fringes in this area are somewhat disturbed (Fig. 3), either because of ground cracking or because of a small-scale atmospheric disturbance. A nearly identical solution is obtained neglecting the data of this area.

The collapse component of the dislocation vector is important because it suggests a volcanic origin of the observed deformation. Volume change may be caused by the migration of magma. To test alternative models without volume change, we recalculated the solution constraining the opening component of the dislocation vector to be zero. The best fitting shear fault is a predominantly normal fault (model B in Table 1), extending less far under Lake Karum than model A (Fig. 3). The rms is 7.87 mm versus 7.50 mm for model A. We also examined constraints on the other components of the dislocation vector (Table 1). For zero strike-slip component (model C) the data fit almost equally well as model A, but not for zero dip-slip component (model D), nor for zero dip-slip and strike-slip components (pure collapse, model E). All best fitting dislocations have similar orientation, indicating that this is a robust feature of the inversions. We also tried to fit the data using Mogi models (models F and G) but obtained a worse fit than using dislocation models (Table 1).

Since phase-unwrapping errors and atmospheric disturbances result in correlated, non-gaussian errors we don't have an objective measure to test whether the difference of 0.37 mm in rms between models A and B is significant. We stay with the subjective statement that model A "fits better" than model B. In the next section we provide geological arguments to support magmatic interaction implied by model A.

Discussion and Implications

The detection of ground deformation around Gada 'Ale is significant because it is located at the tip of the Erta 'Ale range. It may be associated with northward propagation of the range. Three observations suggest that the event has been a repeated phenomenon. First, the deformation closely follows a local topographic low of ~20 m (Fig. 4D); second the subsidence occurred at the lowest part of the Danakil Depression on the margin of a normal-fault bounded lake; third, preliminary inspection of 4 m spatial resolution Corona satellite imagery suggests that lava flows have been tilted such that their flow directions are now upslope. These observations indicate that geothermal events are not the cause of the deformation.

Several reasons suggest a local, volcano-tectonic origin of the observed deformation. First, a model invoking volume change due to magma migration fits the data better than a shear fault. Second, most tectonic structures in the Danakil are oriented rift-parallel NNW [*Barberi and Varet,* 1970] but

Table 1. Modeling parameters

	Location[1]			Dimension[2]		Orientation[2]		Dislocation vector[3]				
Model	East [km]	North [km]	Depth [km]	Length [km]	Width [km]	Dip [°]	Strike [°]	Strike-slip [cm]	Dip-slip [cm]	Opening [cm]	ΔV^4 [10^6 m^3]	rms[5] [mm]
A unconstrained	1.7	3.2	0.2	2.7	1.8	36	32	4	18	-9	-0.43	7.50
B shear fault	1.5	2.6	0.4	1.4	3.2	40	27	4	37	n/a	n/a	7.87
C no strike-slip	1.5	3.0	0.3	2.1	2.0	36	29	n/a	20	-8	-0.34	7.52
D no dip-slip	2.0	3.2	0.2	2.3	1.0	41	56	24	n/a	-21	-0.46	7.71
E opening only	1.6	3.0	0.5	1.9	1.1	22	49	n/a	n/a	-18	-0.38	8.09
F one Mogi source	1.6	2.3	0.7								-0.082	9.69
G two Mogi sources		2.6	0.8								-0.052	8.07
		2.3	0.6								-0.040	

n/a: Parameter constrained zero in inversion.

[1] Center of upper edge of dislocation relative to lower left corner of Fig. 3 at 13°57.25'N,40°27.5'W.

[2] Along-strike length, down-dip width; strike measured clockwise from N, dip measured towards right from horizontal.

[3] Displacement of down-thrown block relative to up-thrown block. Negative opening represents collapse.

[4] Dislocation: product of fault length, width and opening; Mogi source: $3\,a^3\,\Delta P/4\,\mu$, with a radius of sphere, ΔP pressure change, μ shear modulus.

[5] rms=sqrt($\Sigma_i r_i^2/N$) with r_i residuals between data and model prediction, N=619 number of data points.

the observed deformation (and the best-fitting models) are oriented nearly rift-perpendicular NNE. The third piece of evidence comes from the stress regime. The least principal compressive stress is likely rift-perpendicular ENE. Because the tensile strength in rift zones is small (*Haimson and Rummel* [1982] measured 1-6 MPa in Iceland), little traction would be resolved in slip direction of the NNE oriented normal fault suggested by the modeling (model fault B, Table 1). Fault movement could be activated only if the friction on the fault is somehow reduced, for example by magmatic fluids.

Although our preferred model is a combination of normal faulting and collapse on one dislocation surface a combination of distinct sources may be more realistic but the small signal does not warrant such complexity. For example, the withdrawal of magma from a reservoir may have induced normal faulting on a weak zone near the reservoir (leaky fault). The magma reservoir may be located beneath the fault at depth where liquid magma can be maintained without solidifying (~ 2 km). Inspection of Corona images dating back to 1965 and of the coherence map indicates no new lava flows in the area. However, magma may have erupted under Lake Karum. It is unlikely that the observed deformation is related to salt tectonics because we see subsidence and not uplift.

Erta 'Ale. Erta 'Ale volcano reaches 600 m altitude in the center of the eponymous range and has a 1.5 km long summit caldera. The 1993-1997 interferogram lacks any phase signature to indicate shallow magma migration (Fig. 5). The fringes near the caldera are probably atmospheric artifacts because similar phase signatures are found throughout the interferogram. The lack of deformation is surprising because other active basaltic shield volcanoes (e.g., Galapagos and Hawaii) have experienced rapid surface deformation in response to magma migration [*Owen et al.,* 2000; *Jonsson et al.,* 1999]. It suggests that magma accumulation at Erta 'Ale occurs at slower rates and/or greater depth. The lack of deformation is also surprising because Erta 'Ale had an active lava lake during the interferogram period [*Oppenheimer and Francis,* 1998]. It last overspilled in 1972-1974. The continuous supply of fresh, hot magma from a deeper reservoir and the removal of the cooled, degassed magma can maintain the mass and thermal balances of active lava lakes for decades [*Francis and Oppenheimer,* 1993, *Harris et al.*, 1999]. The lack of surface deformation suggests that the cooled lava does not intrude into the countryrock or into the rift zone [suggested by *Harris et al.,* ibid.] but that it descends to a deeper reservoir where it is reheated or emplaced as cumulates.

Conclusions

We have reported an aseismic crustal deformation event near Gada 'Ale volcano in the lowest part of the Danakil Depression. Elastic dislocation modeling indicates a combination of dip-slip and collapse on a shallow source. The volume change together with the rift-perpendicular orientation of the source suggests a local, volcano-tectonic origin of the observed deformation. The event has repeated over geologic time and may be related to the northward propagation of the Erta 'Ale range.

Although the available data do not allow conclusive constraints on the nature of the observed deformation, this study is a further example of how spaceborne radar interferometry can detect volcanic deformation in remote, unpopulated areas where no deformation has previously been observed.

Acknowledgements. This study was supported by a Post-Doctoral grant of the European Space Agency (ESA) to Amelung, and by NASA. SAR data were provided by ESA. We thank reviewer F Sigmundsson for helpful comments. This is SOEST contribution 5226 and HIGP contribution 1110.

References

Amelung F., D. Galloway, J. Bell, H. Zebker, and R. Laczniak, Sensing the ups and downs of Las Vegas: InSAR reveals structural control of land subsidence and aquifer-system deformation, *Geology*,27,483-486, 1999.

Barberi, F. and J. Varet, 1970, The Erta 'Ale volcanic range, *Bull. Volc*, 34, 848-917.

Cervelli, P., M. Murray, P. Segall, Imaging deformation sources with geodetic data, *J. Geophys. Res.*, in press

Chu, D. and R.G. Gordon, Current plate motions across the Red Sea, *Geophys. J. Int.*, 135, 313-328, 1998.

Francis, P., C. Oppenheimer, and D. Stevenson, Endogenous growth of persitently active volcanocs, *Nature*, 366, 554-557, 1993.

Haimson, B. C. and F. Rummel, Hydrofracturing stress measurements in the Iceland research drilling project drill hole at Reydarfjördur, Iceland, *J. Geophys. Res.*, 87, 6631-6649, 1982.

Harris, A., L. Flynn, D. Rothery, C. Oppenheimer, and S. Sherman, Mass flux measurements at active lava lakes: implications for magma recycling, *J. Geophys. Res.*, 104, 7117-7136, 1999.

Manighetti I., P. Tapponnier, V. Courtillot, and S. Gruszow, Propagation of rifting along the Arabia-Somalia plate boundary: The Gulfs of Aden and Tadjoura, *J. Geophys .Res.*, 2681-2710, 1997.

Massonnet, D. and Feigl, K., Radar interferometry and its application to changes in the Earth's surface, *Rev. Geophys.*, 441-500, 1998.

Massonnet, D. and Sigmundsson, F., Remote sensing of volcano deformation by radar interferometry, *Remote Sensing of Active Volcanism*, AGU Mono., ed.: P. Mouginis-Mark et al, 207-221, 2000.

Oppenheimer C. and Francis P., Implications of longeval lava lakes for geomorphological and plutonic processes at Erta 'Ale volcano, north Afar, *J. Volc. Geotherm. Res.*, 80, 101-111, 1998.

Okada Y., Surface deformation due to shear and tensile faults in a half space, *Bull. Seimol. Soc. Am.*, 75, 1135-1154, 1985.

Owen, S., P. Segall, M. Lisowski, A. Miklius, M. Murray, M. Bevis, and J. Foster, January 30, 1997 eruptive event on Kilauea, Hawaii, as monitored by continuous GPS, *Geophys. Res. Lett.*, in press.

Jonsson, S., F. Amelung, H. Zebker and P. Segall, Rapid uplift of Galapagos volcanoes observed with InSAR. Abstr. *Eos, Trans.*, 46, p. 1194, 1999.

Sigmundsson, F., Tectonic implications of the 1989 Afar earthquake sequence, *Geophys. Res. Lett.*, 19, 877-880, 1992.

Tarantola, A., J.C. Ruegg, and J.C. Lepine, Geodetic evidence for rifting in Afar: a brittle elastic model of the behaviour of the lithosphere, *Earth Plant. Science Lett.*, 45, 435-444, 1979

Tapponier, P, R. Armijo, I. Manighetti, and V. Courtillot, Bookshelf faulting and horizontal block rotations between overlapping rift zones in southern Afar, *Geophys. Res. Letts.*, 17, p.1-4, 1990.

White, R.S. and McKenzue, D., Magmatism at rift zones: the generation of volcanic continental margins and flood basalts. *J. Geophys. Res.*, 94, 7685-7729, 1989.

Zebker, H., F. Amelung, and S. Jonsson, Remote Sensing of Volcano Surface and Internal Processes using Radar Interferometry, *Remote Sensing of Active Volcanism*, AGU Monograph, ed.: P. Mouginis-Mark et al, 179-205, 2000.

F. Amelung, Hawaii Institute of Geophysics and Planetology, University of Hawaii, 2525 Correa Rd. Honolulu, HI, 96822, USA (amelung@pgd.hawaii.edu).

C. Oppenheimer, Department of Geography, Cambridge University, Cambridge CB2 3EN, England, U.K. (co200@cus.cam.ac.uc).

P. Segall, H. Zebker, Geophysics Department, Stanford University, Stanford, CA 94305, USA (segall or zebker@stanford.edu).

(Received January 14, 2000; revised April 13, 2000;
accepted July 21, 2000.)